

# ON THE RELATION BETWEEN CHROMOSPHERIC AND PHOTOSPHERIC FINE STRUCTURE IN AN ACTIVE REGION

R. KITAI\* and R. MULLER

*Observatoires du Pic-du-Midi et de Toulouse, 65200 Bagnères de Bigorre, France*

(Received 12 October, 1983)

**Abstract.** A comparative study was done on the bright fine structure in the upper photosphere and in the lower chromosphere of an active region. The results are shown in the following: (a) The bright points in the  $H\alpha$  wing are cospatial to the facular points, which confirms the result of Wilson (1981). (b) Some points bright in the  $H\alpha$  wing are associated with the facular granules which have larger sizes than the facular points. (c) The brightness enhancement in the  $H\alpha$  wing is positively correlated to the enhancement in the blue continuum. However, the correlation is not so strong. (d) The moustache points are also cospatial to the facular features. (e) The geometrical shape of a moustache point is like a funnel and diverging upward in the upper photospheric and the lower chromospheric levels.

Some discussions are given on the nature of the heating mechanism of the fine structure based upon these results.

## 1. Introduction

Now a variety of fine structural features are known to be present in the solar atmosphere. Dunn and Zirker (1973) found the filigree in the far wing of the  $H\alpha$ . Mehlretter (1974) discovered the facular points with a narrow band Ca II K filter. Muller (1977), from continuum pictures near the limb, suggested the existence of the facular granules. These observations and other works (Spruit and Zwaan, 1981; Wilson, 1981; Muller, 1983) have revealed the basic characteristics of each structural feature.

However the observational study of the relationship among these fine structural features seems to be scarce. Wilson (1981) suggested that the continuum facular points, the filigree and the calcium bright points found by Mehlretter (1974) are of the same origin, because the patterns of the spatial distribution of the bright points are similar in the Ca II K, Mg  $b_1 + 0.35 \text{ \AA}$ ,  $H\alpha + 1.5 \text{ \AA}$ ,  $H\alpha$  continuum images. Muller (1983) found the continuum facular points in the intergranular lanes from the comparison of continuum images and Ca II K filtergrams.

In this work, we report the results of our comparative study on the bright fine structure observed in an active region. We have analysed four filtergrams taken in  $H\alpha$  (line center),  $H\alpha - 0.5 \text{ \AA}$ ,  $H\alpha - 0.75 \text{ \AA}$ , and CH4308 band filtergram. From the comparison of the spatial distributions of the bright features, we have basically confirmed the work of Wilson (1981). And we show that the moustaches are also related in origin to the facular points or the filigree. They are different manifestations in different layers and in different magnitude of a same phenomenon. Our semi-quantitative correlation analysis on the brightness enhancements suggests us an interesting and characteristic brightness evolution of these fine structural features.

\* On leave from Kyoto University and Hida Observatory, Japan.

## 2. Observation

The observation was performed with the 50 cm refractor at the Pic-du-Midi Observatory on June 28, 1980. An active region (HL No. 16927) near the disk center ( $r = 0.54$ ) was observed with a  $0.5 \text{ \AA}$  bandpass  $H\alpha$  Lyot filter and with a  $10 \text{ \AA}$  bandpass blue filter centered at  $4308 \text{ \AA}$ . We call the pictures taken through the latter filter as  $B$  images or  $B$  filtergrams.  $H\alpha$  (line center),  $H\alpha - 0.5 \text{ \AA}$ ,  $H\alpha - 0.75 \text{ \AA}$ , and  $B$  filtergrams were taken in the observation. We have selected and analysed the best image from a burst of about fifty pictures taken for each filtergram. Four filtergrams used for analysis were observed during a period of 2 min 20 s, and are shown in Figures 1a–d with their times of exposure.

On the passband of the  $4308 \text{ \AA}$  filter, there are numerous molecular lines of CH. The filtergrams through this filter are considered to display the structure in the upper photospheric levels and are used to identify the facular features at Pic-du-Midi Observatory.

A comment is given here on the brightness of the  $H\alpha - 0.75 \text{ \AA}$  filtergram. One can suppose that a bright feature seen in this filtergram does not represent the structure in the lower chromosphere but only reflects a photospheric continuum enhancement through the siderobes of the Lyot filter transmission. However this supposition is not real. If it were real, all the bright features in the  $B$  filtergram would be observed as bright features in the  $H\alpha - 0.75 \text{ \AA}$  filtergram. On Figure 1, we can find many examples which do not agree with the above supposition. This is true if we take into account the effect of overlying absorbing matter on the  $H\alpha - 0.75 \text{ \AA}$  filtergram. So we consider that the bright features in the  $H\alpha - 0.75 \text{ \AA}$  filtergram really represent the structure in the low chromosphere.

## 3. Facular Features and Bright Points Seen in the $H\alpha$ Wing

Figure 1d shows the  $B$  filtergram of the active region. We can see numerous bright points which have much smaller sizes than the ordinary photospheric granules. These are facular points (Mehltretter, 1974; Spruit and Zwaan, 1981; Wilson, 1981; Muller, 1983), and facular granules (Mehltretter, 1974; Muller, 1977). These facular points are distributed around the two sunspots and along the enhanced network. A  $H\alpha - 0.75 \text{ \AA}$  filtergram, which was taken one minute before the exposure of the  $B$  image, is shown in Figure 1(c). The bright features are also prolific in this filtergram and are distributed over the same region as the facular features. A detailed comparison between these two filtergrams has led us to a conclusion that almost all bright points in the  $H\alpha - 0.75 \text{ \AA}$  image are associated with facular features.

### 3.1. CLASSIFICATION OF THE BRIGHT FEATURES IN THE $B$ FILTERGRAM

First, we have selected bright features in the  $H\alpha - 0.75 \text{ \AA}$  filtergram. With the aid of the other filtergrams, we have identified as fine structures as possible we can. On the annular region surrounding the larger spot, the number of bright points amounts to 398. The

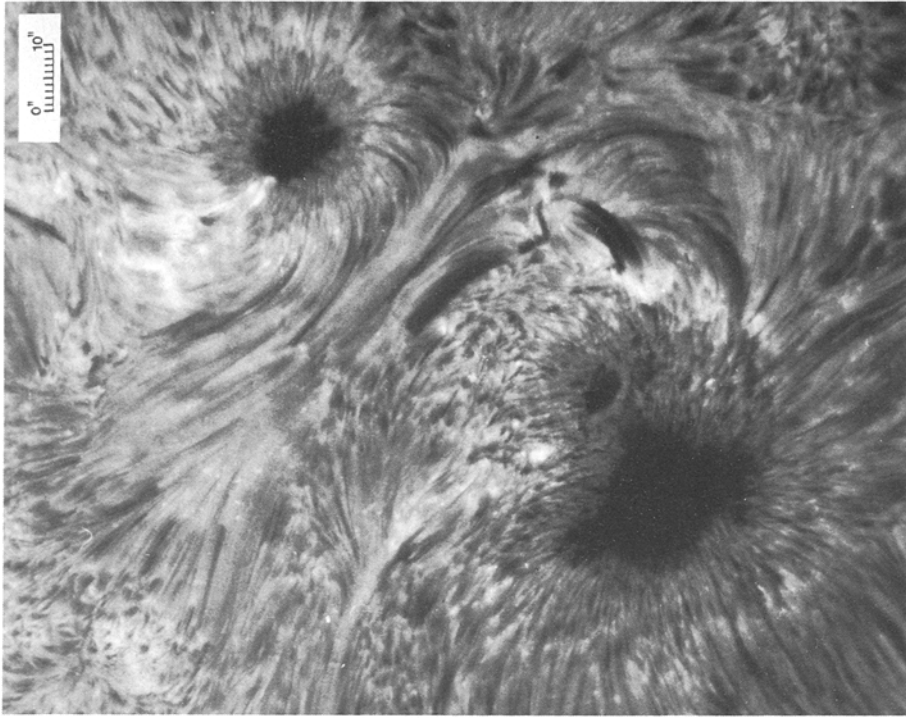


Fig. 1b.  $H\alpha$  - 0.5 Å filtergram at 07<sup>h</sup>54<sup>m</sup>40<sup>s</sup>.

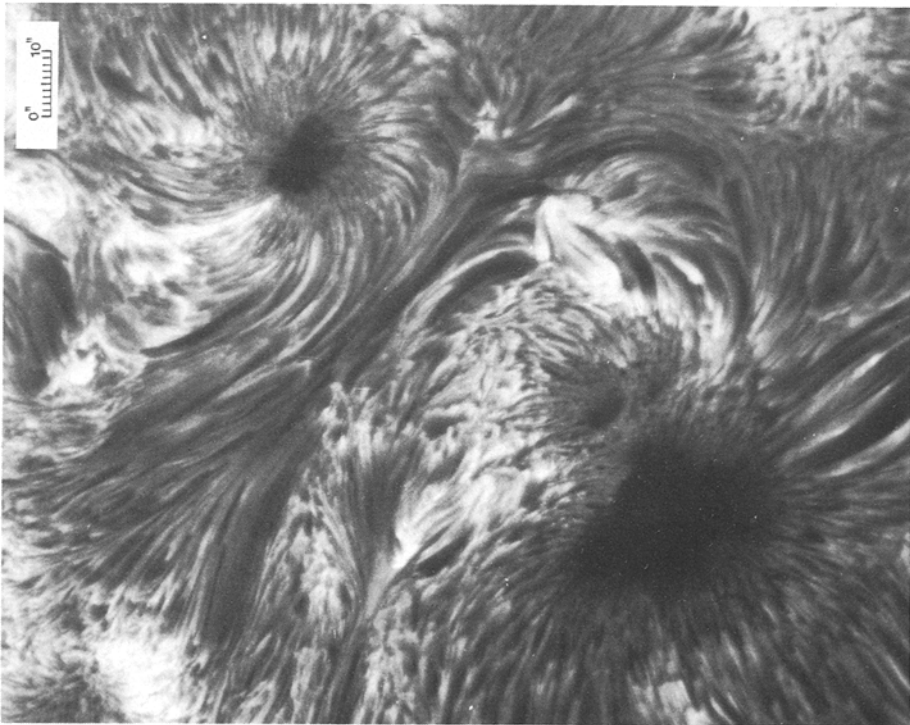
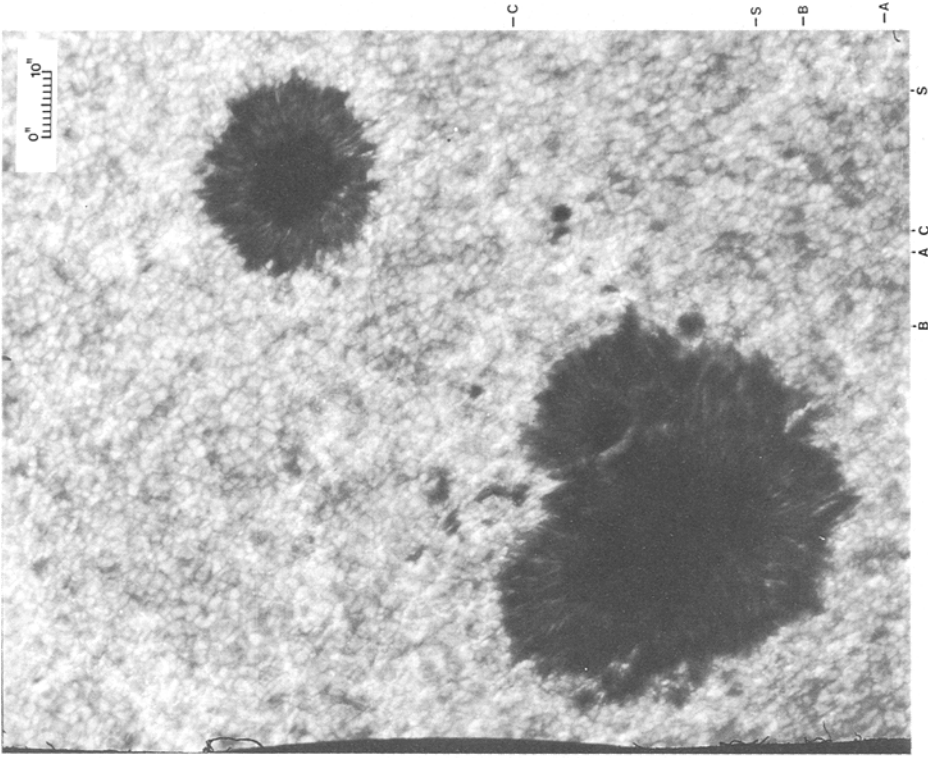


Fig. 1a.  $H\alpha$  line center filtergram at 07<sup>h</sup>52<sup>m</sup>30<sup>s</sup>.



A: Bright facular point. B: Faint facular point. C: Facular granule.  
S: Standard feature used in the brightness classification.

Fig. 1d. B (4308 Å) filtergram at 07<sup>h</sup>54<sup>m</sup>50<sup>s</sup>.

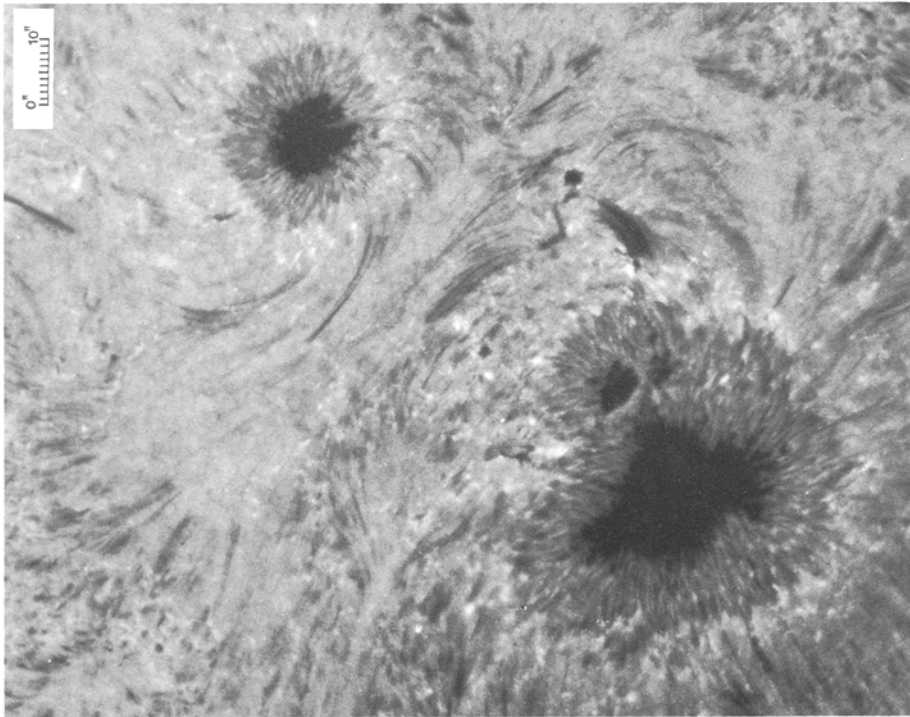


Fig. 1c. H $\alpha$  - 0.75 Å filtergram at 07<sup>h</sup>53<sup>m</sup>50<sup>s</sup>.

annular region just referred is that one which extends outward from the outer edge of the penumbra and has approximately the same width as the penumbral region. On the similar annular region around the smaller sunspot, we have selected 132 bright points. And in the region outside the two annular region, we have identified 346 bright points.

Next we have searched a corresponding facular feature in the *B* filtergram for each bright point in the  $H\alpha$  wing. In the morphological point of view, there is a variety of facular features in the *B* image. On this semi-quantitative work, however, we have discriminated them in their sizes and in their brightness estimated by eye on the print. We have classified them into three classes: (a) bright facular points, (b) facular points with less brightness, and (c) facular granules. The representative points for the three classes are shown in Figure 1d. Small ( $d < 0.5''$ ) compact features have been classified into (a) or (b) depending upon whether they are brighter or not compared to a standard feature. The standard feature is shown in Figure 1(d). On the other hand, we have classified a feature as a facular granule when we can identify a feature with a size  $> 0.75''$ , i.e. comparable to that of the normal photospheric granules and with a somewhat higher brightness, at the corresponding position of the  $H\alpha$  wing feature.

### 3.2. ASSOCIATION OF FACULAR FEATURES WITH BRIGHT POINTS IN THE $H\alpha$ WING

We have classified the bright features in the  $H\alpha$  wing into four classes: (a) associated with a bright facular point, (b) associated with a facular point of less brightness, (c) associated with a facular granule, and (d) not associated with any characteristic features. The histograms of the occurrence of each class are displayed in Figure 3.

From these histograms, we can first notice that about 90% of the bright points in the  $H\alpha$  wing are associated with facular features. This supports the result of Wilson (1981) that the facular points are cospatial with  $H\alpha$  filigree points and are related in origin.

Next, the compact facular points are not the sole associate with bright features in the  $H\alpha$  wing. Although less numerous, the facular granules also associate the  $H\alpha$  wing features. We disagree with Wilson (1981) on this point. As was observed by Dunn and Zirker (1973), these facular granules may correspond to the diffuse phases of the  $H\alpha$  filigree points. However considering that the differences of the occurrence frequency exist between three regions studied by us, we suspect that the facular granules and the facular points are different objects. This can be seen from Figure 2 where we have shown the spatial distribution of the facular granules in the observed region. Facular granules are prolific in active parts. The occurrence frequency of the facular granules seems to depend upon the state of activity of the region (Muller, 1983).

Thirdly, the histograms show that about 10% of the  $H\alpha$  wing features have no corresponding bright features in the *B* image. Partially this may be explained by the difference of the observation time (1 min) between the two filtergrams. However there exist cases where the bright features in the  $H\alpha - 0.75 \text{ \AA}$  can be seen bright in the  $H\alpha - 0.5 \text{ \AA}$  filtergram which was taken virtually simultaneously with the *B* filtergram. Thus some  $H\alpha$  wing features really have no counterparts in the photosphere. This point will be discussed in the next subsection.

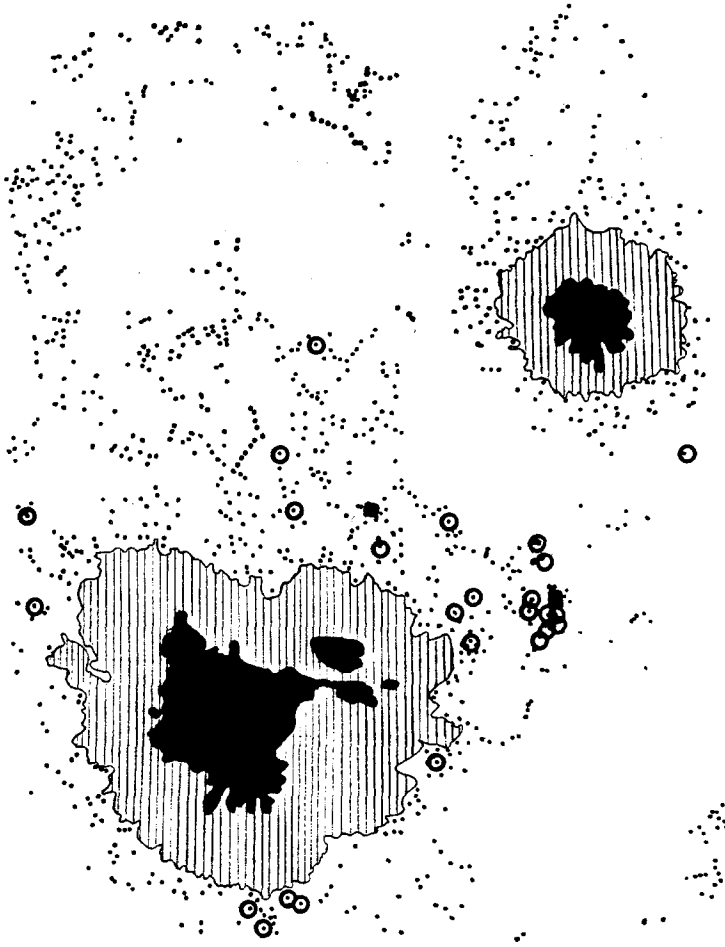


Fig. 2. Spatial distribution of the bright points in the  $H\alpha - 0.75 \text{ \AA}$  filtergram. Small dots indicate the location of the bright points. The bright points associated with facular granules are indicated by encirclements.

Finally, we notice that the relative occurrence of the four classes in the region around the smaller sunspot differs significantly from the others.

### 3.3. RELATION BETWEEN $\Delta I_{H\alpha - 0.75}$ AND $\Delta I_B$

As can be seen in Figures 1c and d, the brightness enhancement in the  $H\alpha - 0.75 \text{ \AA}$  filtergram ( $\Delta I_{H\alpha - 0.75}$ ) is not necessarily proportional to the brightness enhancement in the  $B$  filtergram ( $\Delta I_B$ ). We have studied the correlation between  $\Delta I_{H\alpha - 0.75}$  and  $\Delta I_B$  semi-quantitatively for the features enhanced in the  $H\alpha$  wing brightness. We exclude those features associated with the facular granules in this subsection. We have classified the enhancements in the  $B$  brightness into three ranks, 'bright', 'faint', and 'not enhanced', according to the classes (a), (b), and (d) described in the previous subsection.

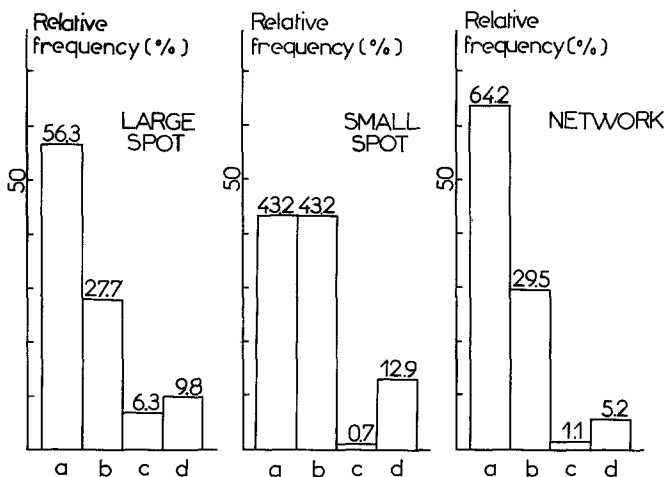


Fig. 3. Relative occurrence frequencies of the four classes of the  $H\alpha - 0.75 \text{ \AA}$  bright points. Four classes are: (a) associated with a bright facular point, (b) associated with a facular point of less brightness, (c) associated with a facular granule, and (d) not associated with any characteristic feature. We have divided the observed region into three sub-regions. Relative occurrence frequencies are obtained for each sub-region.

By estimating visually the  $\Delta I_{H\alpha - 0.75}$  in a similar way to  $\Delta I_B$ , we have classified the enhancements in the  $H\alpha$  wing brightness into two ranks: 'bright' and 'faint'. The results of the classification are summarized in Table I where the number of features in each class is shown.

TABLE I  
Occurrence number of the fine features in 2-dimensional classification by  $\Delta I_{H\alpha - 0.75}$  and  $\Delta I_B$

Around the larger spot			Around the smaller spot				
bright	53	71	bright	11	46		
faint	62	48	faint	26	31		
not enhanced	14	25	not enhanced	11	6		
$\Delta I_B$	$\Delta I_{H\alpha - 0.75}$	faint	bright	$\Delta I_B$	$\Delta I_{H\alpha - 0.75}$	faint	bright

Table I shows that the  $\Delta I_{H\alpha - 0.75}$  is positively correlated to the  $\Delta I_B$  but the correlation is not so strong. There exist 'bright'  $H\alpha$  wing features with 'faint' or 'no'  $B$  enhancements and *vice versa*. The number of these features is not negligible and their existence cannot be considered to be due to some observing conditions. The difference of the observing time of 1 min between the two filtergrams will be negligible compared to the lifetime of facular points (18 min; Muller, 1983). The seeing effects will not be the origin because we can see these features adjacent to bright features in both filtergrams.

We can speculate two alternative possibilities to explain the correlation in Table I. First there may be some phase differences between the evolution in the upper photosphere and that in the lower chromosphere. The possible evolutionary paths in the  $\Delta I_{H\alpha-0.75} - \Delta I_B$  diagram are shown in Figure 4a. If this is real, we can get an important clue to the heating mechanism of the solar features. Following the brightness evolutions in both filtergrams, we may determine the propagation characters of the heating sources (Liu, 1974; Kitai, 1983). The other possibility is that the energy deposition may take place in more or less localized layers. And there may be cases where only the photosphere or the chromosphere are heated. On this hypothesis, the brightness evolution of the features will take the paths in the  $\Delta I_{H\alpha-0.75} - \Delta I_B$  diagram as shown in Figure 4b.

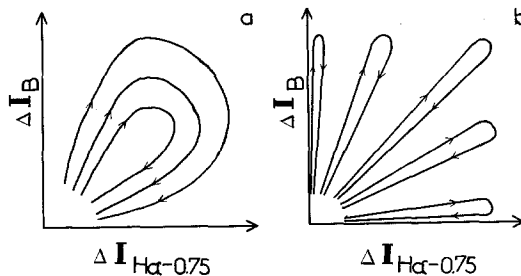


Fig. 4. Illustration of the evolutionary paths of the bright features in  $\Delta I_{H\alpha-0.75} - \Delta I_B$  diagram. (a) Phase difference hypothesis. (b) Local heating hypothesis. The directions of arrows are taken arbitrarily.

Unfortunately our observation cannot discriminate which hypothesis is real, although the first possibility seems to be supported by the observation of Vorpahl and Pope (1972). This point will be discussed further in the next section in relation to the moustache points.

#### 4. Moustaches

The bright points seen in the  $H\alpha - 0.75 \text{ \AA}$  image can be identified as moustaches when they do not show so much brightness in the  $H\alpha$  line center image. The bright points in the  $H\alpha$  wing seen around the sunspots are generally moustaches. Except the upper right quadrant of the larger sunspot in Figure 1, almost all the bright points in the  $H\alpha$  wing around the sunspots are located in the region where dark superpenumbral filaments run radially from the sunspots in the  $H\alpha$  line center image. These moustache points show relatively less brightness in the  $H\alpha$  wing compared with the moustaches in the active part of the larger sunspot. The latter brighter moustaches are usually observed and analysed.

##### 4.1. ASSOCIATION OF FACULAR POINTS WITH MOUSTACHES

Following the discussion of the previous section, we can say that about 90% of the moustaches are associated with facular features, more specifically, with facular points.



Bruzek (1972) found that moustaches are associated with 'facular granules' from his observations near the limb. If we take into account the difference of the spatial resolution, we can state that our observation near the disk center confirms his finding and that the association is confirmed for much fainter moustaches than those observed by Bruzek.

However it must not be disregarded that there exist moustaches which have no corresponding bright features in the  $B$  filtergram. For example, two moustaches, features  $A$  and  $B$  in Figure 5, show similar brightness in the  $H\alpha - 0.75 \text{ \AA}$  filtergram, but only  $A$  is associated with a bright feature in the  $B$  filtergram. This is real and not due to the difference of the observation time, because we can see the bright features for both moustaches in the  $H\alpha - 0.5 \text{ \AA}$  filtergram which was taken virtually simultaneously with the  $B$  image. Two possibilities described in Section 3.3 are relevant for the explanation of this fact.

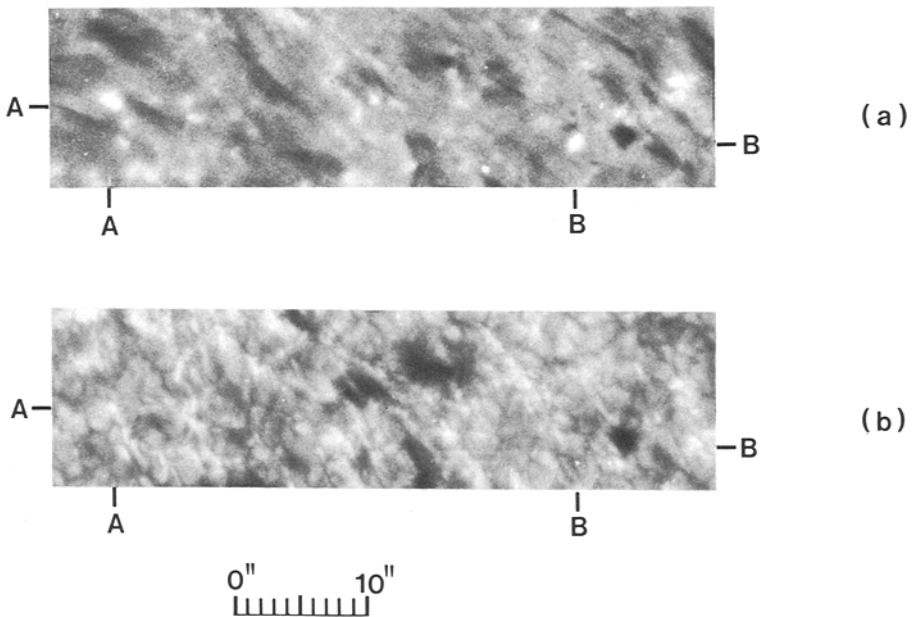


Fig. 5. Examples of bright moustaches. (a)  $H\alpha - 0.75 \text{ \AA}$  image. (b)  $B$  (4308  $\text{\AA}$ ) image. Notice that the moustache  $A$  is associated with a facular point but the moustache  $B$  is not.

Vorpahl and Pope (1972) observed bright moustaches around an emerging flux region. They followed their evolution in 3840  $\text{\AA}$  filtergrams and in  $H\alpha$  off-band filtergrams, and found that the brightness variation in 3840  $\text{\AA}$  leads that one in the  $H\alpha$  wing by  $3.5 \pm 1 \text{ min}$ .

Thus we can suppose that not only the brightness of the bright moustaches in the active parts but also the faint moustaches in the quiet parts around the sunspots may evolve with some phase difference between the photosphere and the chromosphere.

#### 4.2. GEOMETRICAL SHAPE OF A MOUSTACHE POINT

We have selected ten moustache points which are brighter and have larger sizes. These moustache points are associated with facular features. The area of each moustache point is obtained by measuring the length and the width on the printed image and simply by multiplying the two quantities. In Figure 6, we show the relation between the area measured on the  $B$  filtergram and the one measured on the  $H\alpha - 0.75 \text{ \AA}$  filtergram. Clearly the area on the  $H\alpha - 0.75 \text{ \AA}$  image is larger than that on the  $B$  image. The former is about twice of the latter. This indicates that a moustache point has a geometrical shape

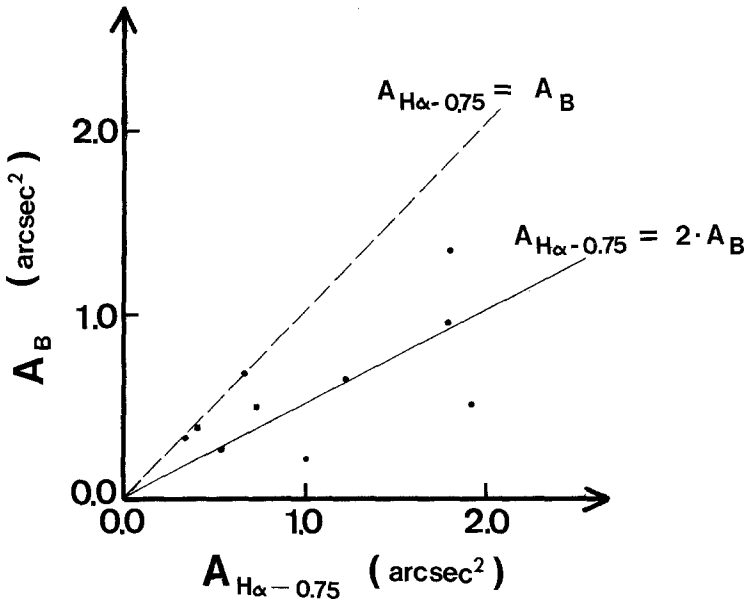


Fig. 6. Scatter plots of  $A_{H\alpha-0.75}$  (area measured on the  $H\alpha - 0.75 \text{ \AA}$  image) and  $A_B$  (area measured on the  $B$  (4308  $\text{\AA}$ ) image).

like a funnel, diverging upward in the layers from the upper photosphere to the lower chromosphere.

As the name shows, when we look at a  $H\alpha$  spectrum of a moustache, the size of the emission region measured along the slit direction decreases as we see from the inner wing to the outer wing of the profile. The form of the emission region in a  $H\alpha$  spectrum tapers toward the outer wavelengths. So far we have been unable to discern the reality of the tapering of the spectrum, because it may be the result of the image blurring due to atmospheric motions. Now from our observation we can state that the tapering of the  $H\alpha$  spectrum is real and that it reflects the geometrical shapes of the moustache point.

#### 5. Discussion and Conclusions

Kitai (1983) showed that a moustache profile can be produced when a hot ( $\Delta T = 1500 \text{ K}$ ) and dense ( $\rho/\rho_0 = 5$ ) condensation is formed in the lower chromosphere.

And with the results of Suematsu *et al.* (1982), he discussed that an abrupt heating at the photospheric levels of an intense and isolated magnetic flux tube may be the origin of a moustache. The association with the facular features and the geometrical shape of the moustaches found in this work, strongly support the previous speculation.

Rust (1968) suggested that the magnetic field reconnection at the magnetic neutral points may be the origin of moustaches as the bright moustaches are frequently observed in newly emerging, changing magnetic regions. However, as our observation shows, moustaches occur not only in the active parts but also in the more or less quiet part of active regions, where it seems to be no opposite fields to be reconnected. Thus we consider that the magnetic reconnection is not the origin of moustaches; rather a heating of an elementary flux tube is relevant. The heating may be active in newly emerging flux tubes.

In conclusion, we have confirmed that in an active region almost all the bright features in the  $H\alpha$  wing are associated with facular features in the upper photosphere. The filigree is known to show enhanced brightness even in  $H\alpha - \frac{5}{8} \text{ \AA}$  filtergrams (Dunn and Zirker, 1973). They are cospatial with facular features (Wilson, 1981). So the faint moustaches observed by us around the sunspots can be supposed to be the same phenomenon as the filigree. We suggest that the faint moustaches, the filigree and the facular points have a common physical origin and that they occur not only in network regions but also in active regions. The bright moustaches, which occur mainly in active parts of an active region, have some different characters compared with the faint moustaches or the filigree. The bright moustaches have diverging geometrical shapes, while the diameter of filigree points increases only weakly along height (Dunn and Zirker, 1973; Spruit and Zwaan, 1981). The bright moustaches have larger sizes than the faint moustaches, although for facular points the smaller is the size, the higher is the brightness (Spruit and Zwaan, 1981). The characters of the heating of an elementary flux tube may depend upon the size of the tube (Spruit and Zwaan, 1981) and its geometrical shape.

To reveal the evolution and the true nature of the phenomena, a time-series observation in chromospheric and photospheric lights with a high angular resolution is eagerly needed.

### Acknowledgements

This work was done during a stay of one of the authors (R.K.) at Pic-du-Midi Observatory. He expresses his hearty thanks to the director J. P. Zahn and all the staff members of the observatory for their kind hospitality during his stay. We are grateful to Dr C. J. Macris who made the  $H\alpha$  filter of the Athens Observatory available to us, and to Dr G. Ceppatelli from Arcetri Observatory who participated in the observations.

### References

- Bruzek, A.: 1972, *Solar Phys.* **26**, 94.  
 Dunn, R. B. and Zirker, J. B.: 1973, *Solar Phys.* **33**, 281.  
 Kitai, R.: 1983, *Solar Phys.* **87**, 135.

- Liu, S. Y.: 1974, *Astrophys. J.* **189**, 359.  
Mehlretter, J. P.: 1974, *Solar Phys.* **38**, 43.  
Muller, R.: 1977, *Solar Phys.* **52**, 249.  
Muller, R.: 1983, *Solar Phys.* **85**, 113.  
Rust, D.: 1968, in K. O. Kiepenheuer (ed.), 'Structure and Development of Solar Active Regions', *IAU Symp.* **35**, 77.  
Spruit, H. C. and Zwaan, C.: 1981, *Solar Phys.* **70**, 207.  
Suematsu, Y., Shibata, K., Nishikawa, T., and Kitai, R.: 1982, *Solar Phys.* **75**, 99.  
Vorpahl, J. and Pope, T.: 1972, *Solar Phys.* **25**, 347.  
Wilson, P. R.: 1981, *Solar Phys.* **69**, 9.